



Eastern boreal North American wildfire risk of the past 7000 years: A model-data comparison

Christelle Hély,¹ Martin P. Girardin,² Adam A. Ali,³ Christopher Carcaillet,³ Simon Brewer,¹ and Yves Bergeron⁴

Received 21 April 2010; revised 4 June 2010; accepted 17 June 2010; published 31 July 2010.

[1] We present here a 7000-year wildfire reconstruction based on sedimentary charcoal series from five lakes located south of Hudson Bay in eastern boreal North America. The reconstruction shows a significant downward trend in the frequency of large fires from 0.0061 fire-yr⁻¹ ca. 5000 cal yr BP to 0.0033 fire-yr⁻¹ at present. Simulations of fire-season climate based on UK Universities Global Atmospheric Modelling Programme output and reconstructions based on proxy data both indicate a shift toward increasing available moisture in the region between the mid-Holocene and today. We infer that the diminishing trend in wildfire activity was ultimately caused by the steady orbitally driven reduction in summer insolation. Future higher temperatures not compensated for by significant precipitation increases will bring fire frequency back toward its upper limit, recorded between 6000 and 2000 cal yr BP.

Citation: Hély, C., M. P. Girardin, A. A. Ali, C. Carcaillet, S. Brewer, and Y. Bergeron (2010), Eastern boreal North American wildfire risk of the past 7000 years: A model-data comparison, *Geophys. Res. Lett.*, 37, L14709, doi:10.1029/2010GL043706.

1. Introduction

[2] Recent extreme wildfire years across North America and Eurasia have raised awareness of potential human-caused effects on this disturbance agent. Notably, large fires increased strikingly in the mid-1980s in the western United States [Westerling *et al.*, 2006], northwestern Canada [Stocks *et al.*, 2002], and at the end of the 20th century in Russia [Conard *et al.*, 2002]. The onset of higher Canadian fire activity in the 1970s compared with previous decades, partly attributed to forcing by changes in atmospheric greenhouse gas concentrations [Gillett *et al.*, 2004], may have marked the end of a 150-year period of diminishing fire activity driven by natural climate forcing [Girardin and Mudelsee, 2008]. The long-term diminishing trend is nevertheless disputed by some authors [e.g., Ter-Mikaelian *et al.*, 2009], mainly because mechanistic explanations (supported by empirical data and model simulation) for the diminishing fire activity have not been forthcoming. Confounding factors such as changes in land use or fire sup-

pression [Marlon *et al.*, 2008] are often used as counter-arguments for rejecting the climate forcing on long-term fire activity. Here we use fire frequency (FF) reconstructions of the past 7000 years based on lake-sediment charcoal and climate information from simulations using general circulation models (GCMs), and reconstructions from paleoclimatic (proxy) data to provide evidence of the imprint of climate on long-term changes in fire activity in eastern boreal North America.

2. Study Area

[3] The study area is contained within the Canadian boreal forest, south of Hudson Bay (auxiliary material).⁵ The vegetation is dominated by black spruce (*Picea mariana* (Mill.) B.S.P.), along with jack pine (*Pinus banksiana* Lamb.). The postglacial vegetation history inferred from pollen records indicates that the vegetation matrix has remained in a stable state during the past 7000 years [Richard, 1995], following the rapid forest expansion after the disappearance of the proglacial Obijbway Lake ca. 8200 calibrated years before present (hereafter BP) [Barber *et al.*, 1999]. Fire history reconstructed from aerial photographs, archives, and dendroecological data suggest that the fire cycle (average time for the area to burn completely) has shifted from 92 years prior to AD1850, to 360 years after AD1920 [Bergeron *et al.*, 2004]. While fire suppression, changes in land use, and landscape fragmentation may have contributed to an unprecedentedly low burn rate in recent decades, diminishing fire activity has also been detected on lake islands on which fire suppression has never been conducted, and provides an argument in support of climate control [Bergeron, 1991].

3. Data and Models

[4] Holocene FF was reconstructed using charred particles (“charcoal”) extracted from the sediments of five small kettle lakes (auxiliary material). These lakes are in close proximity (ca. 100 km), allowing us to minimize potential variability induced by spatial variability of environmental conditions and to better decipher the role of external forcing on FF. We applied the most recent advances in charcoal treatment and statistical analysis [Higuera *et al.*, 2009] to reconstructing fire events over the past 7000 years from charred areas. A kernel-density function [Mudelsee *et al.*, 2004] was used to compute local FF for each core based on its reconstructed fire events (Figure 1), and a mean regional FF (RegFF) based on pooled fire events from all

¹CEREGE, UMR 6635, Université Aix-Marseille, CNRS, Europôle de l’Arbois, Aix-en-Provence, France.

²Canadian Forest Service, Sainte-Foy, Québec, Canada.

³CBAAE, UMR 5059, EPHE, Université Montpellier 2, CNRS, Montpellier, France.

⁴Department of Applied Sciences, Université du Québec en Abitibi-Témiscamingue, Rouyn-Noranda, Québec, Canada.

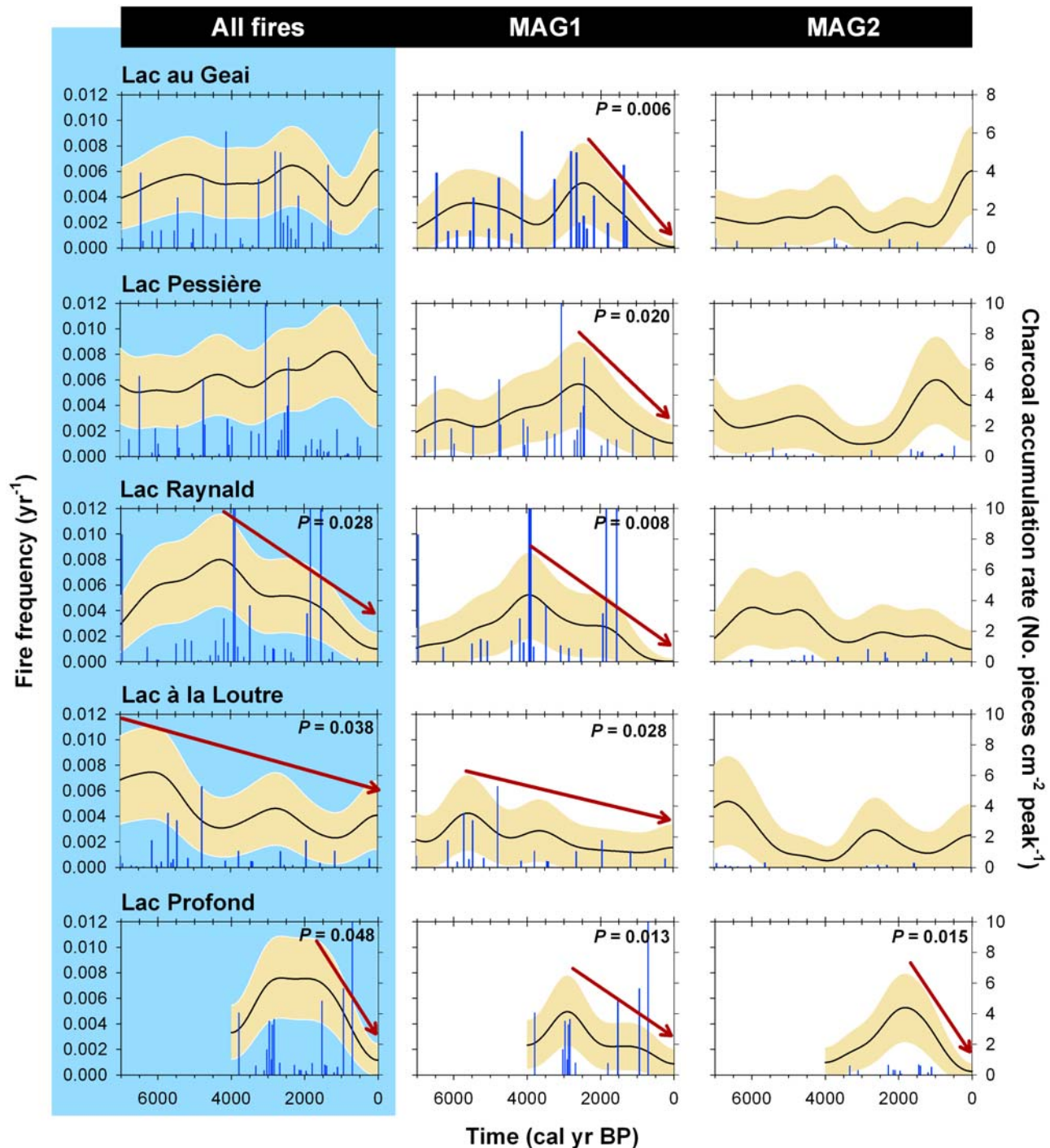


Figure 1. (left) Fire frequencies (FF; thin black lines, left axis) with 90% bootstrap confidence interval (BCI; shaded area) inferred from lacustrine sedimentary charcoal from five Canadian kettle lakes. Fire-event dates are represented as vertical bars with charcoal accumulation rate (right axis). Arrows pointing downward indicate the significant decreasing trend in FF between a given maximum and present, according to the *Cox and Lewis* [1966] statistical test (cf. *P*-values). FF reconstructions after partitioning charcoal peaks into (middle) high- (MAG1) and (right) low- (MAG2) magnitude components using the median charcoal peak accumulation rate of all samples as a criterion.

lakes (Figure 2) with correction for temporal changes in the number of lakes using $RegFF_{(t)} = FF_{(t)}/n_{(t)}$, where $n_{(t)}$ is the number of sampled cores at time t . Significance of temporal changes in local and regional FF was illustrated (Figures 1 and 2) using bootstrap confidence intervals (hereafter BCIs).

[5] The size distribution of boreal fires is distinctly bimodal, with a disproportionately low number of fires accounting for much of the area burned [Johnson and Wowchuk, 1993]. Large-fire years occur under low moisture conditions in deep organic layers driven by mid-tropospheric blocking high-pressure systems that operate on

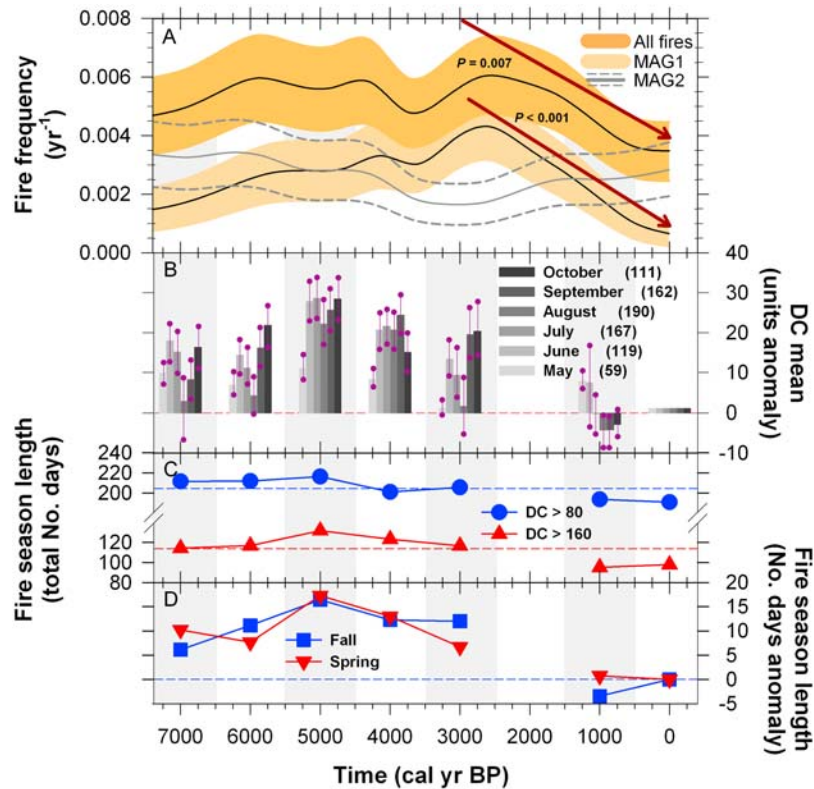


Figure 2. (a) Reconstructions of mean regional fire frequencies (RegFF), (b) monthly means of daily Drought Code (DC), (c) fire-season length and (d) spring and fall departures during the Holocene. RegFF were obtained after pooling fire-event dates from all kettle lakes (Figure 2a). DC departures (with 90% BCI) from the 1901–2002 reference period, with present-day means indicated in parentheses (Figure 2b). Fire-season length assessed from the number of days with simulated DC values higher than 80 and 160 units (moderate and high wildfire risks, respectively) (Figure 2c). Long-term means are indicated by dashed lines. Holocene departure (in days) of fire-season start (spring) and end (fall) for moderate and high wildfire risks (Figure 2d). Figure 2a is obtained from paleodata and Figures 2b–2d from UGAMP simulations.

a regional scale (100- to 1000-km wide). The connection between mid-tropospheric blocking events and large and severe fires has previously been of interest in explaining large spatial-scale synchronicity in FF [Johnson and Wowchuk, 1993]. Starting from these principals, we partitioned fire events into their high- (MAG1) and low- (MAG2) magnitude peaks using the median charred area peak value as the threshold, allowing kernel density estimation using a sufficient number of fire events in each sub-population. We thus hypothesized that MAG1 fires, owing to their higher charcoal influx, should represent severe or large fire events, controlled by large-scale climate processes, within the potential charcoal source area [Higuera *et al.*, 2007]. We are aware that several studies have indicated that distance from a fire may also control peak magnitude [Higuera *et al.*, 2007]. Thus, small peaks could be large fires at a distance from the lake, and large peaks could actually be small fires on the lakeshore. Nevertheless, we think that a reasonable case can be made for interpreting the large peaks as large local fires.

[6] We used paleoclimatic simulations provided by the UK Universities Global Atmospheric Modelling Programme (hereafter UGAMP) [Hall and Valdes, 1997] to develop a mechanistic understanding of the climatic variations associated with the reconstructed FF (auxiliary material). A downscaling method was conducted by applying the UGAMP anomalies of temperature and precipitation to the

Climate Research Unit climatology data set TS 2.1 [Mitchell and Jones, 2005]. Richardson's [1981] weather generator was applied to the simulated time series of monthly temperature and precipitation to derive daily values necessary to compute the Drought Code (DC) index of the Canadian Forest Fire Weather Index System [van Wagner, 1987]. The DC represents the moisture content of organic matter that is on average ~ 18 cm thick and $25 \text{ kg}\cdot\text{m}^{-2}$ dry weight, for a bulk density of $138.9 \text{ kg}\cdot\text{m}^{-3}$. A DC value of zero is indicative of saturation and values higher than 400 are indicative of potential deep burning of sub-surface heavy fuels. The DC is a significant predictor of area burned and number of fires in the study area [Bergeron *et al.*, 2010], explaining 37% and 56% of their annual variance over the period 1959–1999, respectively (auxiliary material). A comparison among six GCM simulations for 6000 BP within our study region showed that simulated July DC range obtained from UGAMP simulation was not significantly different than that from the others (auxiliary material). One should note that we limited our discussion to the period after 6000 BP since UGAMP simulations, as in the case with other GCM simulations, did not take into account the residual Laurentide Ice-Sheet estimated at up to $100\,000 \text{ km}^2$ in extent at 6000 BP (Figure 3 and auxiliary material). The omission of this feature from the GCMs is believed to create simulations in our area that are biased toward warmer conditions at 7000–6000 BP. For all 1000-yr Holocene

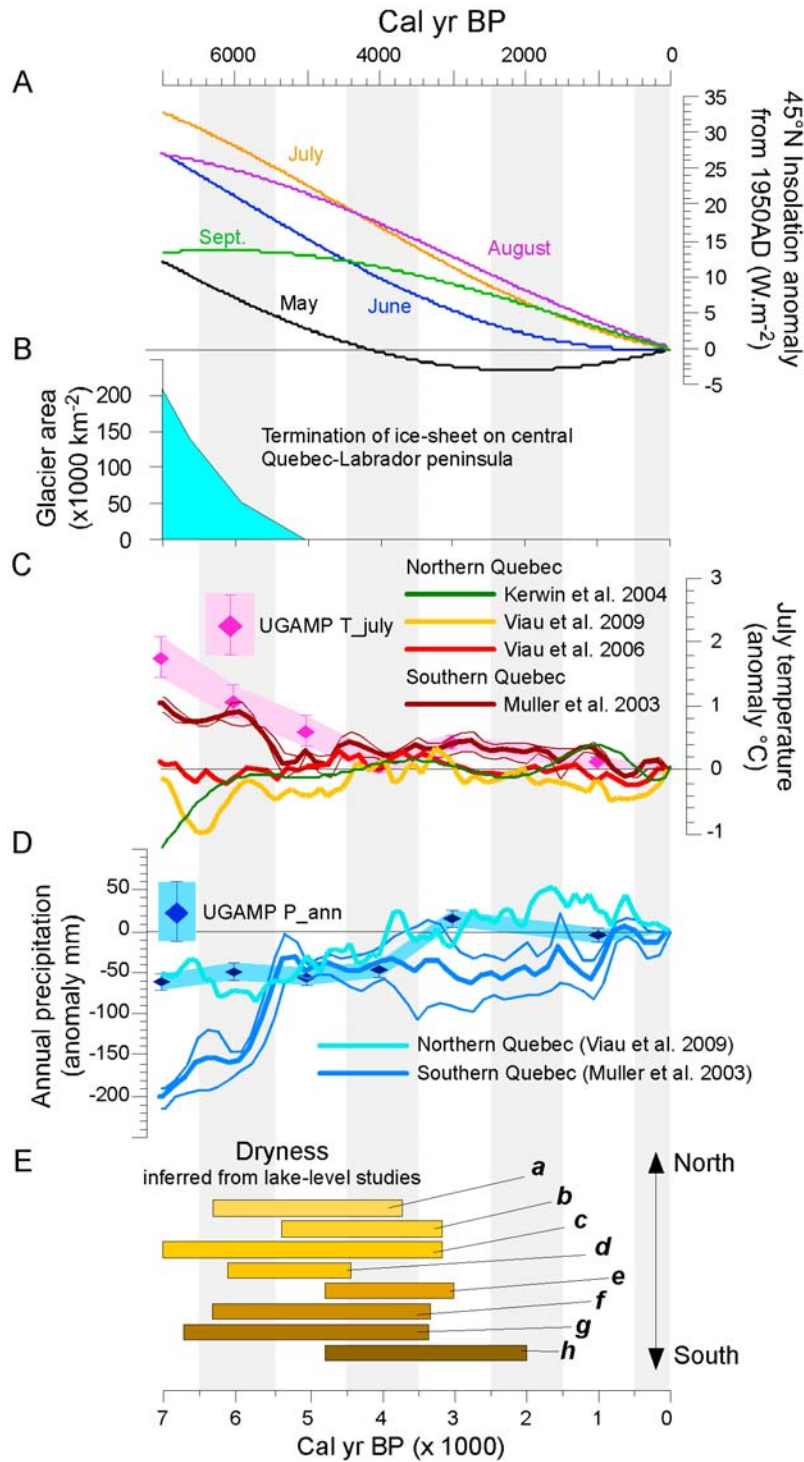


Figure 3. Climate controls, temperature, precipitation and dryness reconstructions (anomalies relative to present-day data) from climatic indicators and UGAMP simulations. (a) Insolation computed at 45°N [Berger and Loutre, 1991]; (b) termination of the Laurentide Ice Sheet inferred from ice-sheet areas [Dyke et al., 2003]; (c) July temperature departures from the 1901–2002 reference period inferred from pollen data and simulated by UGAMP (with 90% BCI); (d) Annual precipitation departures from the 1901–2002 reference period inferred from pollen data for southern and northern Quebec and simulated by UGAMP (with 90% BCIs). (e) Dryness periods inferred from low lake-level status from several studies in eastern Canada (a–h) plotted from the north (yellow/light-brown, southern Hudson Bay) to the south (dark-brown, southeastern Ontario). See auxiliary material for references and interpretations.

periods, we used UGAMP 100-yr daily time series to calculate the mean July DC index and the length of the fire season (auxiliary material), and compared these with the RegFF reconstructed from 6000 BP to the present.

4. Reconstructed Holocene Fire Frequencies

[7] Reconstructed FF from MAG1 peaks of individual lacustrine cores display a coherent decreasing trend starting sometime between 4000 and 2500 BP (Figure 1, middle). MAG1 FF reached a maximum of $0.005 \text{ fire}\cdot\text{yr}^{-1}$ ($\sim 200 \text{ yr}$ for fire return interval, FRI) between 6000 and 1000 BP and declined in average to below $0.002 \text{ fire}\cdot\text{yr}^{-1}$ (FRI $\sim 500 \text{ yr}$) at present. The present-day inter-lake variability is nonetheless high, with current MAG1 FF ranging from 0 to $0.006 \text{ fire}\cdot\text{yr}^{-1}$. However, MAG1 FF for the lakes as a group varies more temporally than it does spatially at any given time. All trends visually identified from MAG1 peaks passed *Cox and Lewis'* [1966] significance test (Figure 1). Unlike with MAG1 peaks, FF inferred from MAG2 peaks and from all peaks did not show coherent patterns among the five lakes. We infer that the composite pattern of small fires be related to climate promoting more local-scale events that are less effective in reducing fuel moisture over large areas.

[8] The present-day (0 BP) RegFF (Figure 2) was estimated at $0.0033 \text{ fire}\cdot\text{yr}^{-1}$ with 90% CI [0.0023, 0.0044], which corresponds to a fire year every 300 yr (90% CI [226, 429]). This value is in the range of known FF in this area, based on dendrochronological investigations [*Bergeron et al.*, 2004], and it is significantly lower than the maxima recorded between 5000 and 2000 BP, according to BCI's and *Cox and Lewis'* [1966] test. Similarly, the MAG1 RegFF confirmed the overall decreasing pattern with a minimum at present, this minimum being significantly lower than at any other time since 7000 BP. The RegFF of MAG2 peaks showed no evidence of a temporal trend (Figure 2). The common trend in MAG1 FF among all five lakes (Figure 1) supports the idea of a control by large-scale or coherent climate variations throughout the period considered in this study.

5. Comparison With GCM Simulations

[9] The RegFF inferred from charcoal, and the length of the fire season, estimated by the number of days with simulated DC values higher than 80 units (auxiliary material), display strong correlation (Figure 2; $r = 0.72$, $P_{(\text{two-sided})} = 0.066$; $N = 7$). The lowest frequency of MAG1 fires occurs between *ca.* 1000 and 0 BP and corresponds to the shortest fire season simulated over the last 6000 years: the number of days when $\text{DC} > 80$ units shifts from $206 \text{ days}\cdot\text{yr}^{-1}$ *ca.* 3000 BP to $191 \text{ days}\cdot\text{yr}^{-1}$ at present, i.e., a decrease of 7%. These differences between past and present-day fire-season length were related both to an earlier onset of the fire season in spring (by 2–5 days), and a later termination in fall (up to 12 days *ca.* 3000 BP). Length of season under high fire risk ($\text{DC} > 160$, auxiliary material) shows a similar pattern of changes (Figure 2). These trends with the longest fire season and the highest RegFF occurring *ca.* 3000 BP were likely related to the higher air temperature in fall and during the year at that time (auxiliary material). Holocene drought severity assessed by mean July DC computed using UGAMP simulations also decreased through the last

6000 years, falling from 189 DC units (90% BCI [177, 201]) at 4000 BP to 167 DC units (90% BCI [159, 176]) today (Figure 2). We estimated from the historical relationship between DC and area burned in our region (auxiliary material) [also see *Bergeron et al.*, 2010] that a shift in mean July DC of such magnitude could translate into an increase in average fire cycle from 214 yr at 4000 BP to 519 yr today. The close correspondence between RegFF reconstructed from MAG1 fires and DC estimated using the UGAMP simulations suggests that inferred changes may illustrate a decrease in the frequency of drought-induced severe and large fires from 6000 BP to the present.

6. Comparison With Independent Proxies

[10] We used fire-independent climate proxies from our region to determine whether the climate-based simulation of the fire season was reasonable (Figure 3). These proxies include July mean temperature and total annual precipitation reconstructed from pollen, and dryness reconstructed from low-level lake status inferred from bio- and geo-proxies (auxiliary material). Such records might not always be the best indicators of fire-driving climatic conditions: the temperature records used herein are indicators of both night- and daytime temperatures, while fire risk is essentially dependent on daytime temperatures [*van Wagner*, 1987]. A similar problem occurs with total annual precipitation because fire risk in our area is mainly dictated by summer droughts [*Bergeron et al.*, 2010]. Nevertheless, these records provide both independent evidence for climate changes in eastern North America, and a basis for evaluating the performance of the UGAMP simulations.

[11] Reconstructions of regional July mean temperature suggest that before 5500 BP air temperature was lower than present in northern Quebec (Figure 3c), but $\sim 1^\circ\text{C}$ higher than present in southern Quebec [*Muller et al.*, 2003]. Such positive anomaly prior to 5500 BP may be explained by the small effect of the residual ice-sheet on the southern region. From 5500 BP to present, all temperature reconstructions show small fluctuations of anomalies compared with the present-day temperature. In contrast, annual precipitation showed important variations over the past millennia (Figure 3d), with a dry period from 7000 to 4000 BP followed by a millennial trend toward wetter conditions, particularly in the north. Long-term changes in both July mean temperature and total annual precipitation were reproduced by the GCM simulations, suggesting that the UGAMP model realistically simulates climate over our area. However, the UGAMP simulations of summer temperature are likely too warm prior to 5000 BP, as they are not affected by the missing residual ice-sheet (Figure 3b and auxiliary material), which would have created colder conditions than would be expected if only insolation acted on the July temperatures (Figure 3a). Reconstructions of dryness or low lake levels (Figure 3e), which take into account both the effect of moisture depletion via evapotranspiration and moisture recharge via precipitation and runoff, are also in agreement with our record of RegFF and the simulated fire-season length (Figure 2). The dry period between 7000 and 3200 BP matches well the long period of high RegFF and long fire season, whereas the last 2000 years are characterized by a clear decrease in RegFF and an increase in water levels. Long-term changes in fire risk calculated using the

UGAMP simulations are partially explained by changes in insolation (Figure 3a). The period from 5000 to 4000 BP was a pivotal period between the mid-Holocene (7000–6000 BP) characterized by very high positive anomalies in spring and fall insolation, and the late-Holocene (3000–1000 BP) marked by an ongoing decrease toward the present. The higher insolation during the 6000–5000 BP period was responsible for higher daytime air temperatures in summer than present (auxiliary material) inducing higher DC values, whereas decreasing late-season insolation and the shift to negative anomalies in May explains lower DC and shorter fire season length over the last 2000 years. Prior to 4000 BP, spring and annual precipitation were lower than present (Figure 3d and auxiliary material), and this also contributed to increasing the fire risk calculated using the UGAMP simulations.

7. Conclusion

[12] Our data indicate that long-lasting periods of high FF have characterized the eastern boreal forests over the past millennia and that these periods are linked to long-term climate changes driven by the changes of orbital forcing. If increased fire activity in eastern Canada is a natural response to warmer climates than at present, then any trend toward higher temperatures not compensated for by significant precipitation increases in the future could lead to an increase in the fire risk over eastern boreal North America. Bergeron *et al.* [2010], using ensemble mean simulations from 19 GCM experiments driven by various scenarios of greenhouse gas emissions, showed that by the end of the 21st century, future July DC levels could increase by ~25 DC units in comparison with the present climate, which are levels similar to those simulated using the UGAMP model for the mid-Holocene. Such rise in DC is predicted to shift the fire cycle from a current (1959–1999) value of 500 yr to 220 yr by the end of the 21st century [Bergeron *et al.*, 2010]. The projected warming trend associated with increasing concentrations of greenhouse gases in the atmosphere will seemingly induce a change in fire risk superimposed on the one already induced by orbital changes, but opposite in sign. This will bring FF back toward the upper limit of its historical range, recorded from 6000–2000 BP.

[13] **Acknowledgments.** We thank the 61^{ème} Commission permanente de coopération franco-québécoise (CLIMAFEUX project) and the CNRS (BOREOFIRE project) for funding this study, *Natural Resources Canada* for providing Holocene ice-sheet extent maps, the PMIP-Project for the GCM simulations, Paul Valdes for the UGAMP outputs, and Manfred Mudelsee for the XTREND software.

References

- Barber, D. C., et al. (1999), Forcing of the cold event of 8,200 years ago by catastrophic drainage of Laurentide lakes, *Nature*, *400*, 344–348, doi:10.1038/22504.
- Berger, A., and M. F. Loutre (1991), Insolation values for the climate of the last 10 million years, *Quat. Sci. Rev.*, *10*, 297–317, doi:10.1016/0277-3791(91)90033-Q.
- Bergeron, Y. (1991), The influence of island and mainland lakeshore landscapes on boreal forest fire regimes, *Ecology*, *72*, 1980–1992, doi:10.2307/1941553.
- Bergeron, Y., S. Gauthier, M. Flannigan, and V. Kafka (2004), Fire regimes at the transition between mixedwood and coniferous boreal forest in northwestern Quebec, *Ecology*, *85*, 1916–1932, doi:10.1890/02-0716.
- Bergeron, Y., D. Cyr, M. P. Girardin, and C. Carcaillet (2010), Will climate change drive 21st century burn rates in Canadian boreal forests outside of natural variability: collating global climate model experiments with sedimentary charcoal data, *Int. J. Wildland Fire*, in press.
- Conard, S. G., A. I. Sukhinin, B. J. Stocks, D. R. Cahoon, E. P. Davidenko, and G. A. Ivanova (2002), Determining effects of area burned and fire severity on carbon cycling and emissions in Siberia, *Clim. Change*, *55*, 197–211, doi:10.1023/A:1020207710195.
- Cox, D. R., and P. A. W. Lewis (1966), *The Statistical Analysis of Series of Events*, John Wiley, New York.
- Dyke, A. S., A. Moore, and L. Robertson (2003), Deglaciation of North America, *Geol. Surv. Can. Open File 1574*, Nat. Resour. Can., Ottawa.
- Gillett, N. P., A. J. Weaver, F. W. Zwiers, and M. D. Flannigan (2004), Detecting the effect of climate change on Canadian forest fires, *Geophys. Res. Lett.*, *31*, L18211, doi:10.1029/2004GL020876.
- Girardin, M. P., and M. Mudelsee (2008), Past and future changes in Canadian boreal wildfire activity, *Ecol. Appl.*, *18*, 391–406, doi:10.1890/07-0747.1.
- Hall, N. M. J., and P. J. Valdes (1997), A GCM simulation of the climate 6000 years ago, *J. Clim.*, *10*, 3–17, doi:10.1175/1520-0442(1997)010<0003:AGSOTC>2.0.CO;2.
- Higuera, P. E., M. E. Peters, L. B. Brubaker, and D. G. Gavin (2007), Understanding the origin and analysis of sediment-charcoal records with a simulation model, *Quat. Sci. Rev.*, *26*, 1790–1809, doi:10.1016/j.quascirev.2007.03.010.
- Higuera, P. E., L. B. Brubaker, P. M. Anderson, F. S. Hu, and T. A. Brown (2009), Vegetation mediated the impacts of postglacial climate change on fire regimes in the southcentral Brooks Range, Alaska, *Ecol. Monogr.*, *79*, 201–219, doi:10.1890/07-2019.1.
- Johnson, E. A., and D. R. Wowchuk (1993), Wildfires in the southern Canadian Rocky Mountains and their relationship to mid-tropospheric anomalies, *Can. J. For. Res.*, *23*, 1213–1222, doi:10.1139/x93-153.
- Marlon, J. R., J. P. Bartlein, C. Carcaillet, D. G. Gavin, S. P. Harrison, P. E. Higuera, F. Joos, M. J. Power, and I. C. Prentice (2008), Climate and human influences on global biomass burning over the past two millennia, *Nat. Geosci.*, *1*, 697–702, doi:10.1038/ngeo313.
- Mitchell, T. D., and P. D. Jones (2005), An improved method of constructing a database of monthly climate observations and associated high-resolution grids, *Int. J. Climatol.*, *25*, 693–712, doi:10.1002/joc.1181.
- Mudelsee, M., M. Börngen, G. Tetzlaff, and U. Grünwald (2004), Extreme floods in central Europe over the past 500 years: Role of cyclone pathway “Zugstrasse Vb”, *J. Geophys. Res.*, *109*, D23101, doi:10.1029/2004JD005034.
- Muller, S. D., P. J. H. Richard, J. Guiot, J. L. de Beaulieu, and D. Fortin (2003), Postglacial climate in the St. Lawrence lowlands, southern Québec: Pollen and lake-level evidence, *Palaeogeogr. Palaeoclimatol. Palaeoecol.*, *193*, 51–72, doi:10.1016/S0031-0182(02)00710-1.
- Richard, P. J. H. (1995), Le couvert végétal du Québec-Labrador il y a 6000 ans BP: Essai, *Geogr. Phys. Quat.*, *49*, 117–140.
- Richardson, C. W. (1981), Stochastic simulation of daily precipitation, temperature, and solar radiation, *Water Resour. Res.*, *17*, 182–190, doi:10.1029/WR017i001p0182.
- Stocks, B. J., et al. (2002), Large forest fires in Canada, 1959–1997, *J. Geophys. Res.*, *108*(D1), 8149, doi:10.1029/2001JD000484.
- Ter-Mikaelian, M. T., S. J. Colombo, and J. Chen (2009), Estimating natural forest fire return interval in northeastern Ontario, Canada, *For. Ecol. Manage.*, *258*, 2037–2045, doi:10.1016/j.foreco.2009.07.056.
- van Wagner, C. E. (1987), Development and structure of the Canadian Forest Fire Weather Index System, *For. Tech. Rep. 35*, Can. For. Serv., Ottawa.
- Westerling, A. L., H. G. Hidalgo, D. R. Cayan, and T. W. Swetnam (2006), Warming and earlier spring increase western U.S. forest wildfire activity, *Science*, *313*, 940–943, doi:10.1126/science.1128834.
- A. A. Ali and C. Carcaillet, CBAE, UMR 5059, EPHE, Université Montpellier 2, CNRS, 163 rue Broussonet, F-34090 Montpellier CEDEX, France.
- Y. Bergeron, Department of Applied Sciences, Université du Québec en Abitibi-Témiscamingue, 445 boulevard de l'Université, Rouyn-Noranda, QC J9X 5E4, Canada.
- S. Brewer and C. Hély, CEREGE, UMR 6635, Université Aix-Marseille, CNRS, Europôle de l'Arbois, POB80, F-13545 Aix-en-Provence CEDEX, France. (hely@cerege.fr)
- M. P. Girardin, Canadian Forest Service, 1055 P.E.P.S., POB 10380, Sainte-Foy, QC G1V 4C7, Canada.